Neural Networks, Vol. 6, pp. 1045–1059, 1993
Printed in the USA.

0893-6080/93 $6.00 + .00

INVITED REVIEW

Stability Constraints for the Distributed Control of Motor Behavior

MENASHE DORNAY,[1] FERDINANDO A. MUSSA-IVALDI,[2] JOSEPH MCINTYRE,[2] AND EMILIO BIZZI[2]

[1]ATR Human Information Processing Research Laboratories, Kyoto, Japan
[2]Department of Brain and Cognitive Sciences, Massachusetts Institute of Technology

(*Received and accepted* 17 *March* 1993)

Abstract—*We have investigated the relation between static stability of a limb, equilibrium-point control, and the ill-posed problem of coordinating a redundant ensemble of muscles. Geometrically, equilibrium-point control is equivalent to establishing a mapping between the command signals delivered to the muscles and the equilibrium configurations of a limb. A necessary condition for the existence of such mapping is that the limb be stable across the workspace. We analyzed how this condition may be translated into precise biomechanical constraints for single- and multi-joint limbs. The satisfaction of these constraints is necessary for the equilibrium-point hypothesis to be a viable control paradigm. We show how these same constraints are sufficient to insure the successful operation of a distributed algorithm based upon minimization of potential energy that computes the muscle-control signals corresponding to a desired time sequence of equilibrium points.*

Keywords—Equilibrium-point, Arm, Posture, Movement, Stability, Moment-arm, Muscle.

1. INTRODUCTION

By any reasonable definition, a model of how the brain organizes and controls motor behaviors must be capable of dealing with the mechanical properties of limbs and muscles. As it is natural to assume that biological computation is carried out by a massively parallel neural network, it is also quite evident that the mechanical output of biological motor systems is organized in a very large number of small modules, such as the motor units that act simultaneously upon the skeletal apparatus. These elementary neuromuscular modules are the concrete foundation of what has been called "mechanical computation" (Goswami, Peshkin, & Colgate, 1990), that is, the process of coordinating the mechanical properties of a large number of mechanical components in order to achieve a desired behavior of the entire system.

To further pursue the analogy between neural and mechanical computation, one may note that in both cases there is a crucial notion, that of stability, that establishes a linkage between the overall behavior of a distributed system and the performance of each component. For example, in the case of artificial neural networks, a learning algorithm such as back propagation is based upon the existence of a scalar error function with at least one stable minimum. More generally, it has long been recognized (Cohen & Grossberg, 1983; Hopfield & Tank, 1985) that global Lyapunov functions can be used to design and describe the performance of associative memories.

Both the general notion of stability and the Lyapunov functions are generalizations of concepts (such as potential energy) that came to light in the field of mechanics. Hence, it is not surprising that mechanical stability has been proposed as a powerful organizing principle for motor control (Hogan, 1984). Stability is the key concept behind a control paradigm—the *equilibrium-point hypothesis*—that has been developed and has attracted considerable attention over the last 25 years (Feldman, 1966; Kelso & Holt, 1980; Bizzi, Accornero, Chapple, & Hogan, 1984; Hogan, 1984; Mussa-Ivaldi, Hogan, & Bizzi, 1985; Flanagan, Ostry,

Acknowledgements: This work was supported by NIH grants NS09343 and AR26710 and by ONR grant N00014/88/K/0372 to E. Bizzi and F. A. Mussa-Ivaldi, and a Fairchild Fellowship to J. McIntyre. M. Dornay, who worked on this project both at MIT and at ATR, was supported at MIT by NIH fellowship 1-F05-TWO4042-01 and a Fairchild fellowship. M. Dornay would like to thank Drs. M. Kawato, K. Nakane, Y. Tohkura, E. Yodogawa, and K. Habara from ATR for their continuing support.

Requests for reprints should be sent to Menashe Dornay, Department of Applied Mathematics, The Weizmann Institute of Science, Rehovot, Israel.

& Feldman, 1990; Bizzi, Hogan, Mussa-Ivaldi, & Giszter, 1992; Latash, 1992).

Briefly, the equilibrium-point hypothesis is based upon the observation that muscles behave like tunable springs (Rack & Westbury, 1969; Hoffer & Andreassen, 1981). At any fixed level of descending commands, the isometric tension developed by a muscle is a function of the muscle's length. This dependence of muscle force upon muscle length has been observed both in denervated (Rack & Westbury, 1969) and in reflexive (Nichols & Houk, 1976) muscles. Furthermore, the muscles acting upon a joint are organized in agonist/antagonist configurations. Therefore, at any level of neural activation descending upon the motoneurons, a limb's equilibrium position is achieved when the opposing position-dependent torques generated by agonist and antagonist muscles cancel each other. If the limb is displaced by some external perturbation, the elastic muscle properties generate a net restoring torque, which tends to re-establish the original limb's posture. This inherently elastic behavior of muscles is the physical basis for the stability of posture both in single- and multi-joint limbs. Mussa-Ivaldi, Hogan, and Bizzi (1985) and subsequently Shadmehr and Arbib (1992) have experimentally demonstrated that the posture of the multi-joint arm corresponds to a field of forces acting upon the hand and converging to a point in the arm's workspace. A number of investigations (Hogan, 1984; Flash, 1987) have suggested that the central nervous system (CNS) may exploit this stable postural control for generating arm trajectories without having to deal with an inverse dynamics problem.

More recently, Mussa-Ivaldi and coworkers (Mussa-Ivaldi, 1986; Mussa-Ivaldi, Morasso, & Zaccaria, 1988; Mussa-Ivaldi & Hogan, 1991) have also suggested that the stability induced by the muscles' mechanical properties may allow the CNS to solve the ill-posed computational problems related to motor redundancy. In any biological system, the number of muscles (or motor-units) required to execute a given motor task far exceeds the number of coordinates directly specified by the task. Furthermore, muscles and skeletal joints are arranged in geometrical configurations that must satisfy certain noninvertible constraints. The torques generated by the muscles acting upon a joint add up to determine a net joint torque. We call this a common-position constraint because a given joint configuration uniquely determines the lengths of each of the involved muscles. This constraint cannot be directly inverted: A given net joint torque may be generated by an infinite number of muscle force combinations. Similarly, the angular displacements of the shoulder, elbow, and wrist add up (modulo a Jacobian transformation) to determine the net displacement of the hand. This is a common-effort constraint (where *effort* is a general term referring to forces and torques) because a given hand force uniquely specifies the required joint torques. Again, this relationship cannot be directly inverted; a given displacement of the hand can be achieved by a variety of joint angle displacements. Thus, the CNS must simultaneously solve ill-posed computational problems at several levels, mapping hand positions to joint configurations, joint torques to muscle forces, and muscle forces to motor-unit activities.

Mussa-Ivaldi, Morasso, and Zaccaria (1988) have suggested that a simple way to provide unique solution for these ill-posed motor problems is by mimicking passive behaviors. When the environment imposes a displacement to the endpoint of a passive mechanical system—no matter how complex—the laws of physics are sufficient to determine uniquely forces and displacements of all the constituent components—no matter how many. This simple principle has been incorporated in a distributed control algorithm, called "backdriving," that determines the control input to each actuators by simulating the adaptation to an externally imposed displacement (Mussa-Ivaldi, Morasso, Hogan, & Bizzi, 1991). Ultimately, this algorithm is capable of generating multi-joint limb trajectories by establishing time-sequences of equilibrium points. In this investigation we found that local mechanical stability of the entire controlled structure is a crucial factor for this type of algorithm to operate successfully.

More generally, we have studied the fundamental relationship between postural stability, the equilibrium-point hypothesis, and the ill-posed problem of coordinating a redundant ensemble of muscles. We started by considering whether the elastic properties of the muscles (i.e., the inherent stability of each controlled component) may provide a sufficient condition for equilibrium-point control. Our findings indicate that this is not the case: The spring-like behavior of the muscles is not sufficient to ensure the stability of a whole limb at equilibrium. Limb stability is critically influenced by the geometrical arrangement of the muscles and, in particular, by their position-dependent moment arms. In this respect *the equilibrium-point hypothesis is a falsifiable theory:* It is a viable control hypothesis if and only if certain specific geometrical constraints are met by the biological design of the musculoskeletal system. We investigated these geometrical constraints both analytically and by designing mathematical models of single-joint and multi-joint limbs. This analysis provides insight on how the mechanical "design" of a system can offer the sufficient conditions for distributed equilibrium-point control.

2. STATIC STABILITY AND STIFFNESS EIGENVALUES

A limb is at an equilibrium posture when it is at rest and the net torque around the joints is zero. An additional characterization of posture is offered by the concept of static stability. In general, a limb is statically

stable when the pattern of torques induced by an externally-imposed small displacement tends to restore the equilibrium posture. This concept is more rigorously defined by a condition on the stiffness tensor. Let the limb kinematics be described by a set of N generalized coordinates, $q_1, q_2, \ldots, q_N$. With this notation, a configuration of the limb is an array, $q = [q_1, q_2, \ldots, q_N]^T$. Accordingly, a generalized force is the vector $Q = [Q_1, Q_2, \ldots, Q_N]^T$. In a first approximation, biological limbs can be described as open chains of segments connected by rotational joints. In this case, the generalized coordinates are joint angles and the generalized forces are joint torques. The stiffness tensor in generalized coordinates, R, transforms an infinitesimal change of configuration into a change of generalized torque:

$$dQ = Rdq. \tag{1}$$

This tensor is numerically represented by a $N \times N$ square matrix, R:

$$[R]_{i,j} = \frac{\partial Q_i}{\partial q_j}.$$

A necessary and sufficient condition for local stability about an equilibrium configuration is that all the eigenvalues of R have a negative real part (Ogata, 1970). We will restrict our analysis to statically conservative systems.[1] For this type of system, the stiffness tensor is symmetric and has real eigenvalues. Therefore, the requirement of stability is reduced to the condition that all the eigenvalues of R be negative.

The restriction to statically conservative systems is consistent with the observation of symmetry in the stiffness tensor measured during the maintenance of multi-joint arm posture by human subjects (Mussa-Ivaldi, Hogan, & Bizzi, 1985). The symmetry of the stiffness tensor is relevant to the stability of an arm in contact with a mechanically passive environment (Colgate & Hogan, 1989). Loosely speaking, a system is passive when it cannot deliver more energy than that which it has received. Recent theoretical investigations have demonstrated that a necessary and sufficient condition for coupled stability with a passive environment is that the arm itself behaves as a passive system at any fixed value of the motor commands (Colgate, 1988). An arm with a nonsymmetric stiffness would not act as a passive system: It would either absorb or generate mechanical work in a quasi-static cyclical motion.[2]

[1] A system is said to be statically conservative when the generalized force at rest can be expressed as the gradient of a scalar potential function, $U(q)$. This condition is equivalent to requiring that $\partial Q_i/\partial q_j = \partial Q_j/\partial q_i$.

[2] This is a direct consequence of Stokes' theorem. A nonsymmetric stiffness corresponds to a force field with nonzero curl. According to Stokes' theorem, the work around a closed path is given by the net flux of the field's curl across the surface enclosed by the path.

2.1. Stiffness Transformations

Muscles are the controllable source of effort and stiffness for biological limbs. In a static (isometric) condition, muscles and the spinal reflexes that act upon them behave like *tunable springs* (Rack & Westbury, 1969; Hoffer & Andreassen, 1981). At any level of neuromuscular activation, the isometric force developed by a muscle is a function of the muscle's length. For a wide range of physiological lengths, the tension developed by a muscle during a stretch counteracts muscle's elongation ("muscles pull") and increases in amplitude with increasing stretch amplitudes. This behavior is tunable because a change in neural activation affects the length-tension curve smoothly, without drastically changing its shape. Mathematically, these observations are summarized by stating that the isometric tension, f developed by a muscle is a continuous differentiable function of the muscle's length, l, and input, u:

$$f = f(l, u). \tag{2}$$

Also, for a wide range of lengths the muscle stiffness, $k = \partial f/\partial l$ is negative.

Several muscles act on each joint in an agonist/antagonist configuration. Geometrically, the contribution of the muscles to the joint stiffness matrix is derived from a coordinate transformation. Let us consider a set of M muscles operating on N generalized coordinates ($M > N$). The lengths of these muscles define an M-dimensional space in which a generic point is given by the array $l = [l_1, l_2, \ldots, l_M]^T$. The kinematics of the limb determines a value of l for each value of q through the map:

$$l = \phi(q). \tag{3}$$

The local Jacobian of this map, $\mu = \partial\phi/\partial q$, is a rectangular, $M \times N$ matrix whose element i, j defines the moment arm of the ith muscle with respect to the jth joint angle.

Given a vector of muscle forces, $f = [f_1, f_2, \ldots, f_M]^T$, the corresponding joint torque vector, Q, at a configuration q is obtained as

$$Q = \mu(q)^T f \tag{4}$$

Taking into account (a) the dependence of muscle forces upon length [eqn (2)] and (b) the muscle kinematics [eqn (3)], the joint stiffness is derived by applying the chain rule to eqn (4). Symbolically, we may write:

$$R = \frac{\partial Q}{\partial q} = \mu^T \frac{\partial f}{\partial q} + \frac{\partial \mu^T}{\partial q} f. \tag{5}$$

Introducing the $N \times N$ matrix γ,

$$[\gamma]_{i,j} = \sum_{k=1}^{M} \frac{\partial^2 l_k}{\partial q_i \partial q_j} f_k. \tag{6}$$

and the $M \times M$ muscle-stiffness matrix, k,

$$[k]_{i,j} = \frac{\partial f_i}{\partial l_j}, \quad (7)$$

Equation (5) becomes:

$$R = \mu^T k \mu + \gamma. \quad (8)$$

The two terms on the right side of this expression represent, respectively, a linear transformation of the muscle stiffness matrix and a correction term. This last term accounts for the nonlinearity of the muscle-kinematics. The muscle stiffness matrix, k, represents the *explicit* dependency of muscle tension upon muscle length.

The matrix γ represents the "geometric stiffness" induced by the muscle kinematics. Equation (6) shows that this geometric stiffness vanishes in two cases: (a) when the muscle moment-arms are constant (that is when the muscle kinematics is linear) and (b) when all the muscles operate at their rest length (that is when all the f_i's are zero). If neither condition is met, then one should assume that the geometric stiffness provides a significant contribution to the net joint-stiffness. In particular, the geometric stiffness can either increase or decrease the margin of stability determined by the muscle stiffness matrix.

2.2. Computational Consequences of Static Stability

The geometric stiffness plays an important role not only with respect to the control of movements and postures but also with respect to computation. In particular, here we will consider the role of static stability with respect to the equilibrium-point hypothesis (Feldman, 1966; Hogan, 1984). According to this hypothesis, goal-directed movements at moderate speed are planned and implemented by the CNS as time-sequences of stable equilibrium postures. More formally, the equilibrium-point hypothesis can be stated as follows. The net effect of the muscles' spring-like behavior is to induce a static dependency of the joint torque, Q upon the configuration, q and upon the control input, u. That is, by combining the length-tension relations [eqn (2)], the muscle kinematics [eqn (3)], and tension-torque transformation [eqn (4)] one obtains a single map from q and u to Q:

$$Q(q, u) = \mu(q)^T f(\phi(q), u) \quad (u \in \mathcal{U}, q \in \mathcal{Q}). \quad (9)$$

Under precise conditions, the equilibrium equation,

$$Q(q, u) = 0, \quad (10)$$

defines a map, $g(\cdot)$ from the input, u, to an equilibrium configuration, q_0:

$$q_0 = g(u) \quad (11)$$

$$q_0 \in \mathcal{Q} \quad , \quad u \in \mathcal{U} \quad (12)$$

$$Q(q_0, u) = 0. \quad (13)$$

According to the fundamental theorem on implicit functions (Sokolnikoff & Redheffer, 1966) a necessary and sufficient condition for such a map to exist within a region $A \subset \mathcal{Q} \times \mathcal{U}$ is that the determinant of the joint stiffness tensor, $|\partial Q/\partial q|$, is different from zero in A. If one of the stiffness eigenvalues changes its sign at a point P in A, so does the determinant of R, and the map g ceases to be defined at P. In contrast, if all the stiffness eigenvalues remain negative in the entire region, A, then the function g is uniquely defined across that region. In this case, g maps the control variable u into a set of stable equilibria. If the control input is given as a function of time, $u(t)$, then the image of $u(t)$ under g is an *equilibrium trajectory*, that is a time sequence of stable equilibria, $q_0(t)$.

We want to stress that the above discussion refers to multi-joint mechanisms operated by a number of actuators, which may well exceed the number of joints. Thus, the geometrical value of the equilibrium-point hypothesis is given by the possibility of mapping a high-dimensional control vector, u, into a low-dimensional variable that corresponds to a configuration. The condition for such a transformation to exist is entirely expressed by a tensor whose rank cannot exceed the dimension of the configuration space.

Is the equilibrium point hypothesis a necessary consequence of the motor system's spring-like behavior? To answer this question one must take a closer look at eqn (8), which relates the joint stiffness, R, to the muscle stiffness matrix, k. The fact that muscles operate as "pulling springs" can be expressed by stating that throughout the limb configuration space the eigenvalues of the matrix $\mu^T k \mu$ are all negative. However, the net joint stiffness matrix is also influenced by the geometric stiffness, γ, which arises from the variability of the muscles' moment arms.

This geometric stiffness may generate mechanical instability within large regions of a limb's workspace. Within any such unstable regions the equilibrium-point hypothesis is not a viable control scheme for generating movements and for maintaining limb postures. Thus, the equilibrium-point hypothesis *cannot be considered as a mere consequence of the muscles' spring like behavior:* the stability of a limb is affected by a geometrical factor that is not univocally related to the intrinsic muscle mechanics. This conclusion is illustrated by the following single-joint control example.

3. A SIMPLE EXAMPLE

To show how static instability can be induced by geometrical factors let us consider a simple single-joint mechanism (Figure 1): a planar pendulum operated by a pair of opposing springs (S_1 and S_2). The first spring, S_1, is a controllable element whose force-length relation is given by Hooke's law:

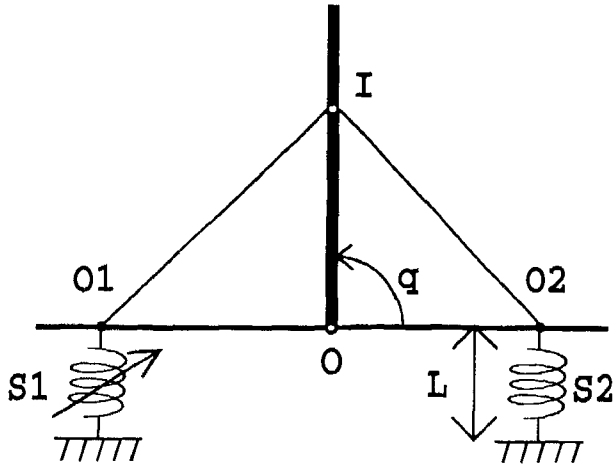

FIGURE 1. A planar pendulum operated by a pair of opposing springs. q is the joint angle of the pendulum.

$$f_1 = K_1(l_1 - u), \tag{14}$$

where K_1 is the stiffness constant and u is the (controlled) rest-length. The second spring, S_2, is also governed by Hooke's law but has fixed stiffness and rest-length parameters K_2 and λ:

$$f_2 = K_2(l_2 - \lambda). \tag{15}$$

In the following discussion we will assume that both springs act as pulling elements and that the constants, K_1 and K_2 are negative. The springs are connected to the pendulum at a common insertion point, I. The length of each spring is the sum of a fixed offset, L, plus a variable segment ($\overline{O_1I}$ and $\overline{O_2I}$). Hence, the muscle-kinematics is given by the equations:

$$l_1(q) = (\overline{OI}^2 + \overline{OO_1}^2 + 2\overline{OI}\,\overline{OO_1}\cos(q))^{1/2} + L \tag{16}$$

$$l_2(q) = (\overline{OI}^2 + \overline{OO_2}^2 - 2\overline{OI}\,\overline{OO_2}\cos(q))^{1/2} + L. \tag{17}$$

For any pendulum configuration, q, the equilibrium condition is:

$$Q(q, u) = \mu_1(q)f_1(l_1(q), u) + \mu_2(q)f_2(l_2(q)) = 0, \tag{18}$$

where we have introduced the moment arms $\mu_1 = \partial l_1/\partial q$ and $\mu_2 = \partial l_2/\partial q$. In this simple system, with a single controlled element, the control variable, u, corresponding to each equilibrium configuration can be derived by replacing the expressions [eqns (14) and (15)] for f_1 and f_2 in eqn (18):

$$u(q) = l_1(q) + \frac{\mu_2(q)K_2}{\mu_1(q)K_1}(l_2(q) - \lambda). \tag{19}$$

Using eqns (8) and (19), the joint stiffness at equilibrium as a function of the angle, q, is:

$$R = \mu_1^2K_1 + \mu_2^2K_2 + \underbrace{\frac{\partial\mu_1}{\partial q}f_1(q, u(q)) + \frac{\partial\mu_2}{\partial q}f_2(q)}_{\gamma}. \tag{20}$$

The last two terms on the right-hand side represent the geometric stiffness, γ, of the joint. Unlike the first two terms, they may assume a positive value and lead to a positive value of R, that is, to an unstable behavior of the pendulum. This case is demonstrated in Figure 2b. The solid line represents the joint stiffness, R, at different equilibrium configurations with the following choice of geometrical and mechanical parameters: $K_1 = -1$, $K_2 = -0.8$, $\lambda = 0.4$, $\overline{OO_1} = \overline{OO_2} = \overline{OI} = 1$, $L = 0.5$. With this choice of parameters, the equilibrium is stable ($R < 0$) at pendulum configurations ranging between 72° and 180°. The joint stiffness is zero at 72° (Figure 2a). Between 72° and 0° the joint stiffness at equilibrium is positive. No fixed value of the control input can be used to maintain a stable posture within this latter range.

The solid line in Figure 2c is a plot of the control variable, u, at different equilibrium angles as derived from eqn (19). This curve has a nonmonotonic shape, with a maximum at 72°. Therefore, the equilibrium configuration cannot be expressed as a single-valued function of u in the entire range of motion of the mechanism. This is a simple illustration of a case in which

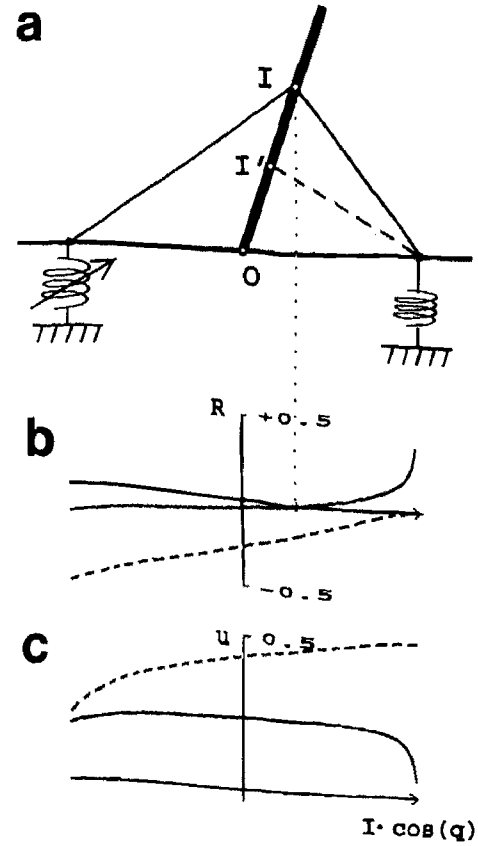

FIGURE 2. Stability analysis of the planar pendulum. R is the joint stiffness, and u is the control input to the tunable (left) spring. The solid lines show that the system is not stable for joint angles from 0° to 72°. The dashed lines show that the system becomes stable when the attachment of the right spring is moved from I to I'.

TABLE 1
The Dissected Muscles

#	Muscle	Origin	Insertion	Function
1	Latissimus dorsi	Vertebrae	Humerus	Shoulder extensor
2	Posterior deltoid	Scapula	Humerus	Shoulder extensor
3	Teres-Major	Scapula	Humerus	Shoulder extensor
4	Teres-Minor	Scapula	Humerus	Shoulder extensor
5	Infra-Spinatus	Scapula	Humerus	Shoulder extensor
6	Pectoralis major capsularis	Clavicula	Humerus	Shoulder flexor
7	Pectoralis major sternalis	Sternum	Humerus	Shoulder flexor
8	Anterior deltoid	Clavicula	Humerus	Shoulder flexor
9	Coraco brachialis	Scapula	Humerus	Shoulder flexor
10	Triceps lateralis	Humerus	Ulna	Elbow extensor
11	Triceps medialis	Humerus	Ulna	Elbow extensor
12	Brachialis	Humerus	Ulna	Elbow flexor
13	Brachio-Radialis	Humerus	Radius	Elbow flexor
14	Pronator teres	Humerus	Radius	Elbow flexor
15	Triceps longus	Scapula	Ulna	2-Joint extensor
16	Biceps brevis	Scapula	Radius	2-Joint flexor
17	Biceps longus	Scapula	Radius	2-Joint flexor

the equilibrium condition in eqn (10) cannot be used to define implicitly a map from the control input to the equilibrium configuration.[3] This result demonstrates that for a simple system operated by spring-like actuators the equilibrium-point control may not be a viable strategy for generating movements and for controlling stable postures.

However, a simple correction of the system's design may lead to a mechanical behavior that is appropriate for the equilibrium-point control. To this end, in our example (Figure 2a, dashed line) it is sufficient to move the insertion of the spring S_2 to a new point, I', which is located midway between O and I ($\overline{OI'} = \frac{1}{2}$). With this geometrical correction, the equilibrium is stable in the entire range of movement (Figure 2b, dashed line) and the control variable is a monotonic function of the equilibrium angle (Figure 2c, dashed line). In the following sections we will apply the same approach to the anatomical analysis of the primate's upper-limb.

4. A PLANAR MODEL OF THE MONKEY'S ARM

In the preceding section we discussed a specific mechanical system that may become inherently unstable by virtue of a geometrical nonlinearity. But, what if, instead of such an artificially simple mechanism, we were to consider a complex multi-joint system, such as a biological limb, operated by a multitude of viscoelastic elements? Is it reasonable to expect that "on the average," the spring-like properties of a large ensemble of muscles are sufficient to remove such apparently occasional instabilities? To address these questions, we have simulated the control of equilibrium postures in a more complex mechanism that incorporated some of the biomechanical characteristics of the primate's arm. The results of our investigation demonstrate that an increase in the system complexity and in the number of spring-like actuators does not lead to better stability properties.

4.1. The Model Structure

4.1.1. *Kinematics.* We considered a two-joint arm, restricted to move only in the horizontal plane. The torso, upperarm, and forearm links were modeled as rigid segments, interconnected by the shoulder and elbow joints. The relative angles of rotation were $q_1 \in [-45°, 90°]$ for the shoulder and $q_2 \in [30°, 135°]$ for the elbow. The kinematics of the model muscles were defined so as to approximate the geometry of the major arm muscles of the rhesus monkey (Table 1). A total of 17 muscles, including shoulder, elbow, and two-joint flexors and extensors have been included in this model. Geometrically, each model muscle acted on a one-dimensional line joining the attachment points. The kinematic constraint imposed by the joint was modeled as a pulley. According to the configuration of the limb, a model muscle could either act on a straight segment between the points of origin and insertion or it could be partially wrapped around the joint pulley (Figure 3).

The kinematics of the hand were described by a pair of cartesian coordinates, x and y, defining the position of the distal extremity of the outer link with respect to

[3] In this case, the fact that the opposite map (from equilibrium angle to input) is defined is merely a consequence of the lack of redundancy in this ad-hoc example: There is a single configuration variable and a single controlled element. If there were more controlled elements than configuration variables (as is the case with musculoskeletal systems) the mapping between q and u would have been ill-defined in both directions.

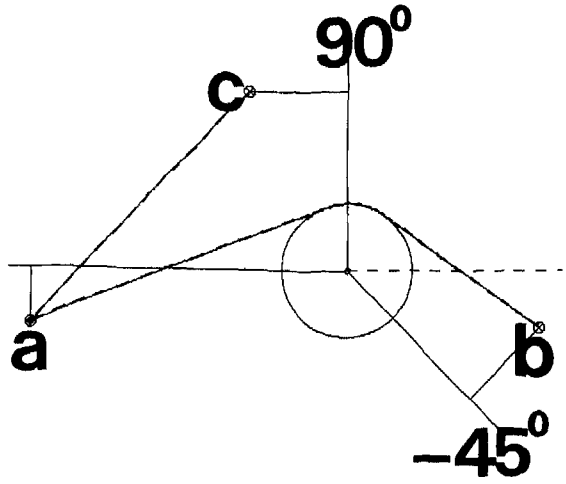

FIGURE 3. Initial geometric model of the shoulder flexor muscle pectoralis major capsularis. The muscle originates from the torso link at (a). The insertion of the muscle to the upperarm link is marked as (b) ($q = -45°$) or (c) ($q = 90°$). The joint angle affects the muscle length and determines whether it is wrapped around its pulley at the joint (b) or is unwrapped (c).

the shoulder joint. These coordinates were derived from the joint configuration, (q_1, q_2), as:

$$\begin{cases} x = l_1\cos(q_1) + l_2\cos(q_1 + q_2) \\ y = l_1\sin(q_1) + l_2\sin(q_1 + q_2) \end{cases}, \qquad (21)$$

where l_1 and l_2 indicate the lengths of the upperarm and of the forearm, respectively.

4.1.2. *Muscle Mechanics.* Mechanically, a prominent feature of muscle behavior at steady-state is the increase of force that results both from an increase in muscle length and an increase in neuromuscular input (Rack & Westbury, 1969; Hoffer & Andreassen, 1981). This mechanical behavior is analogous to that of a tunable spring. In our model, we assumed that the model muscles followed a linear length-tension relationship (Hooke's law) for each value of the control input, u, that is:

$$f = \kappa(u)(l - l_0(u)) \quad u \in [0, 1]. \qquad (22)$$

This is a strong simplification of the actual muscle behavior. However, data obtained by Zeffiro (1986) in the intact behaving monkey, indicate that eqn (22) may be taken as a valid first-order approximation of muscle mechanics for a wide range of muscle lengths.

The joint torque, $Q = (Q_1, Q_2)$, and the joint stiffness,

$$R = \begin{bmatrix} \frac{\partial Q_1}{\partial q_1} & \frac{\partial Q_1}{\partial q_2} \\ \frac{\partial Q_2}{\partial q_1} & \frac{\partial Q_2}{\partial q_2} \end{bmatrix},$$

are derived from the muscle stiffnesses, the muscle operating tensions, and the matrix of moment arms, $[\mu(q)]_{i,j} = \partial l_i/\partial q_j$, as indicated by eqns (4) and (5).

To derive the hand stiffness, K, corresponding to the joint stiffness, R, we took the derivative of the transformation from the joint torque, $Q = (Q_1, Q_2)$, to the hand force, $F = (F_x, F_y)$:

$$Q = J^T(q)F, \qquad (23)$$

where, $J(q)$, is the Jacobian of the kinematic transformation [eqn (21)]. Thus, for those regions where $J(q)$ is invertible:

$$K = (J^T)^{-1}(R - \Gamma)J^{-1} \qquad (24)$$

with

$$\Gamma = \begin{bmatrix} \frac{\partial^2 x}{\partial q_1^2}F_x + \frac{\partial^2 y}{\partial q_1^2}F_y & \frac{\partial^2 x}{\partial q_1 \partial q_2}F_x + \frac{\partial^2 y}{\partial q_1 \partial q_2}F_y \\ \frac{\partial^2 x}{\partial q_1 \partial q_2}F_x + \frac{\partial^2 y}{\partial q_1 \partial q_2}F_y & \frac{\partial^2 x}{\partial q_2^2}F_x + \frac{\partial^2 y}{\partial q_2^2}F_y \end{bmatrix}. \qquad (25)$$

4.1.3. *Control.* The control input to each of the model muscles was a continuous real-valued variable, u, ranging between a "resting" value (0) and a maximum-activation value (1). As indicated by eqn (22), this variable determined uniquely the stiffness and the rest-length of the corresponding model muscle. For the sake of simplicity, we modeled the dependency of the stiffness and rest-length upon the input variables as linear relationships:

$$\kappa(u) = Au + B \qquad (26)$$

$$l_0(u) = Cu + D. \qquad (27)$$

Analysis of muscle behavior suggests that as the activation variable increases from 0 to 1, the stiffness should increase (in absolute value) and the rest-length should decrease, corresponding to muscle shortening (Rack & Westbury, 1969; Zeffiro, 1986).

4.2. Model Parameters

The geometrical and mechanical parameters used in the model were estimated by postmortem dissection of rhesus monkey (*Macaca mulatta*). Planar projections of the arm and shoulder girdle complex were obtained by top-down X-ray imaging of the thoracic cage and arm of the monkey, fixed in a typical configuration used by alive monkeys during horizontal arm movements (Dornay, 1991a, 1991b). The torso link was modeled as an imaginary line segment connecting the two shoulder joints. The upperarm link is an imaginary line segment connecting the shoulder and elbow joints. The forearm link is the line segment passing from the elbow through the wrist to the center of the hand. The lengths of the upperarm and of the forearm links were measured to be 15.5 cm and 20.2 cm, respectively.

TABLE 2
Muscle Parameters

#	Muscle	Origin (cm)	Insertion (cm)	Volume (cm^3)	D (cm)
1	Latissimus dorsi	(−5.5, −10.0)	(2.1, 1.0)	50.0	11.9
2	Posterior deltoid	(0.8, −4.4)	(5.2, 1.5)	21.3	4.28
3	Teres-major	(−0.2, −6.4)	(2.8, 0.5)	25.3	5.35
4	Teres-minor	(0.2, −5.0)	(0.8, 0.6)	4.75	4.87
5	Infra-spinatus	(−0.2, −4.8)	(0.8, 0.6)	26.4	4.76
6	Pectoralis major capsularis	(−4.8, −0.8)	(2.7, 1.5)	37.0	4.76
7	Pectoralis major sternalis	(−5.5, 1.3)	(2.7, 1.5)	33.0	4.19
8	Anterior deltoid	(−2.4, −2.0)	(5.2, 1.5)	15.1	7.18
9	Coraco brachialis	(−1.6, −1.0)	(6.0, 1.5)	4.3	6.90
10	Triceps lateralis	(−12.2, 0.2)	(−0.8, −1.6)	45.8	12.3
11	Triceps medialis	(−5.6, −0.2)	(−0.8, −1.6)	26.5	5.86
12	Brachialis	(−5.7, 0.7)	(2.3, −0.3)	15.2	4.39
13	Brachio-radialis	(−5.0, −0.2)	(16.5, 0.8)	24.4	13.3
14	Pronator teres	(−1.2, −0.5)	(9.3, 0.3)	9.5	8.76
15	Triceps longus	(0.4, −2.2)	(−0.8, −1.6)	45.8	13.6
16	Biceps brevis	(−1.6, −1.0)	(2.7, 0.5)	28.0	14.0
17	Biceps longus	(−0.73, −1.5)	(2.7, 0.5)	26.5	14.6

The muscles listed in Table 1 were exposed and their centers of attachments were marked by drilling holes and gluing metal screws into the bones. The (x, y) coordinates of the muscle attachments were estimated from the X-ray projections of the metal screws. Each model muscle connected a proximal joint with a distal joint. A muscle's origin was referred to a Cartesian system centered at the distal joint. A muscle's insertion was referred to a Cartesian system centered at the proximal joint. For both Cartesian systems, the x axis included the segment joining the proximal to the distal joint (the link axis) and was oriented from proximal to distal. When all the joint angles were 0 degrees, the y axes were all parallel and pointed to the anterior direction. For a more detailed account of the attachment geometry see Dornay (1991a).

From the X-ray projections, we also estimated the radii of the model pulleys around the joints (shoulder, 1 cm for all the muscles; elbow, 1 cm for the flexors, and 1.5 cm for the extensors). The volumes of the muscles were measured by water displacements. Table 2 lists the volumes and the coordinates of attachment for the 17 muscles used in this model.

We used these geometric data to estimate the control parameters A, B, C, and D of eqns (26) and (27). These control parameters were established in three steps. First, we arbitrarily set the minimum rest-length of each muscle (D) to be 99% of its minimum physiological length (Table 2).[4] Second, we estimated the control parameters from the length-tension data obtained by Zeffiro (1986) for the triceps medialis of the intact rhesus monkey (muscle number 11 in our data base). Third, we scaled these triceps parameters according to the rest-lengths and cross-sections of the other muscles. A simplified physiological cross-section, σ (An, Hui, Morrey, Linchield, & Chao, 1981) was calculated for each muscle by dividing its volume by its minimum rest-length. Thus, the control parameters for all the model muscles were computed from the following expressions:

$$A_i = \frac{\sigma_i}{\sigma_{11}} \frac{D_{11}}{D_i} A_{11}$$

$$B_i = \frac{\sigma_i}{\sigma_{11}} \frac{D_{11}}{D_i} B_{11}$$

$$C_i = \frac{C_{11}}{D_{11}} D_i,$$

with $i = 1, \ldots, 17$. The above equations correspond to the hypothesis that muscles are composed of sarcomeres with identical mechanical properties. On one hand, the stiffness of a muscle is directly proportional to the number of sarcomeres in parallel and inversely proportional to the number of sarcomeres in series. On the other hand, at any level of activation, the rest-length of a muscle is given by the sarcomere's rest-length multiplied by the number of sarcomeres in series. The physiological cross-section provides an estimate of the number of sarcomeres in parallel. The number of sarcomeres in series was assumed to be proportional to the minimum rest-length, D.

4.3. The Simulation Algorithms

Simulations of the mechanical behavior of the model were carried out on a software package designed for the Symbolics 3600 Lisp machine (McIntyre, 1990)

[4] That is, the minimum length that could be assumed across the workspace. This setting assured that the muscle always had some (small) residual tension.

which was modified for the tasks at hand (Dornay, 1991a); Given a planar mechanism, this package was designed to solve both direct and inverse statics and kinematics problems. Mathematical details about the algorithms can be found in (Mussa-Ivaldi, Morasso, Hogan, & Bizzi, 1991; McIntyre, 1990). Here, we give a brief qualitative outline of the principles implemented by this software.

Computationally, the arm model consists of a set of equations interacting with two types of input/output processes: the control processes and the environment. On one hand, the control processes specify a set of control variables, u_i, which determine the stiffness and rest-length of each muscle. On the other hand, the environment can act on the system either as an impedance or as an admittance. In the former case, the arm provides a position output to the environment and receives a force input from the environment. In the latter case, the input/output relations between the arm and the environment are reversed: the arm receives a position input and generates a force output. In a direct problem, the control and either the force or the position variables are specified as inputs to the arm. The problem is to determine the other variable as output to the environment. There are then two distinct types of direct problems:

- Given the control and the force variables, determine the position variable. A particular case of this problem is that of finding the equilibrium position corresponding to a given control pattern. In this case, it is implicitly assumed that the environment imposes a constraint of zero force on the model arm.
- Given the control and the position variables, determine the force variable. An example is the problem of finding the force exerted by the hand at a workspace location with a given set of control inputs. A strictly related direct problem is that of determining the stiffness tensor corresponding to given control and position variables.

One important aspect of these direct problems is that they are all well-posed, that is, they can be uniquely solved regardless of the redundancy of degrees of freedom in the model arm.

4.4. The Model Arm Has Unstable Behaviors

To investigate the stability of our model arm, we started by setting all the control parameters [eqns (26) and (27)] to the same value (0.5). With these control parameters, the arm was at equilibrium in the position shown in Figure 4a. Then, while keeping constant the control inputs, we calculated the hand stiffness as a function of the location in the workspace. The dark dots in Figure 4 indicate locations at which the joint stiffness was unstable, while the light dots indicate postures with stable joint stiffnesses. At equilibrium, a necessary and sufficient condition for hand stability is that the joint stiffness be stable (Dornay, 1991b). Away from equilibrium (i.e., when there is an external force), stability depends on the external force as well (Mussa-Ivaldi, Morasso, Hogan, & Bizzi, 1991; McIntyre, 1990). Practically, however, the forces generated in these simulations were low, and there was little effect of the force load. Thus, the overall stability of the limb was determined primarily by the stability of the joint stiffness. It is apparent that with this choice of parameters there was a significant region of instability. Similar unstable regions were observed with other control patterns.

Next, we considered the effect of varying the degree of muscle coactivation upon the size of the unstable region. Figures 4b and 4c, show the regions of instability with all the control parameters equal to 0.2 and 0.8, respectively. As the degree of coactivation increased, so did the region of instability. Contrary to what one might have expected, *coactivation made the limb more unstable.* This counterintuitive finding is explained by observing that the essential source of instability for the arm is the geometric stiffness, γ, in eqn (8). Because muscles always pull ($f_i < 0$), the sign of the components of γ [see eqn (6)] can be either positive or negative according to the sign of the derivatives of the moment arms, $\partial^2 l_k / \partial q_i \partial q_j$. If these derivatives are negative, then the corresponding contributions to γ are positive and the stability margin is decreased. By increasing the activation of a muscle whose moment-arm derivative is negative the margin of stability is further reduced.

Summing up: Our results indicate that (a) with all the tested values of the control parameters, the model arm had a wide region of instability; and (b) the region of instability was increased by increasing the level of coactivation.

4.5. Inverse Problems and the Backdriving Algorithm

Inverse problems arise when one tries to determine the control variables corresponding to given values of both force and position variables at the interface with the environment. For a redundant system such as our model arm, these inverse problems are ill-posed and their solution is not unique. For example, consider the problem of finding the control variables corresponding to a given equilibrium position of the arm. In this case, both the position and the force (zero) at the interface with the environment are specified. It is evident that with a redundant system of muscles, there is an infinite number of control patterns corresponding to the same equilibrium position. In order to derive a unique solution, it is necessary to impose some extra constraint, such as an optimization principle.

We tested a specific optimization principle, the *backdriving* algorithm, which corresponded to a process of adaptive control. Briefly, backdriving the arm from a current equilibrium position to a new equilibrium

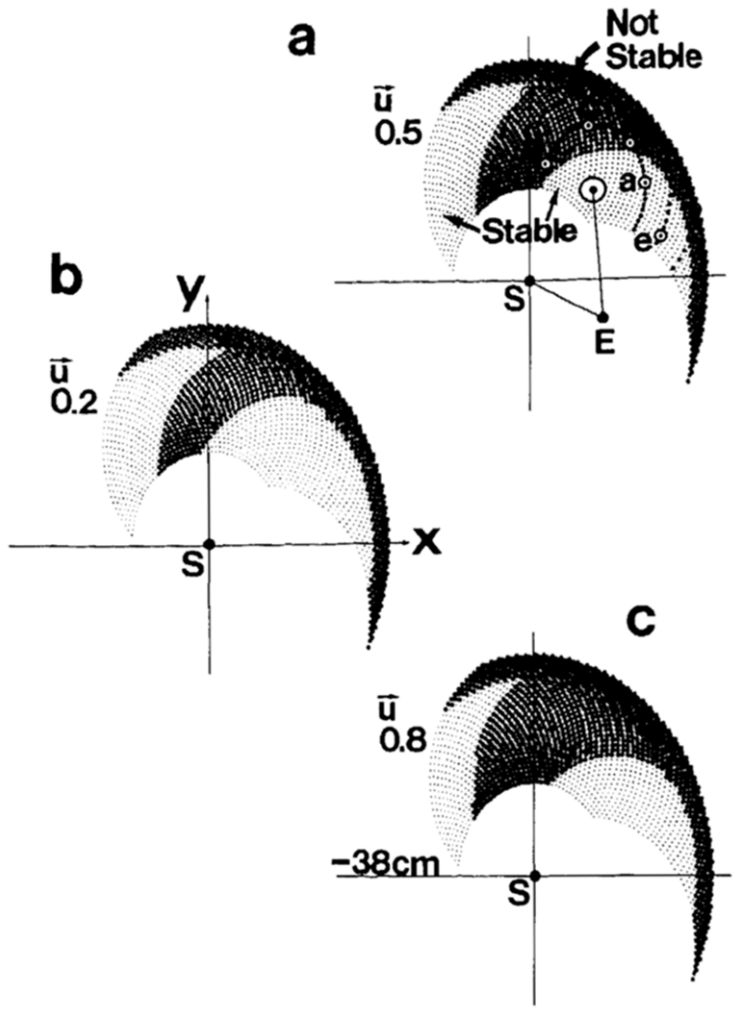

FIGURE 4. Initial hand stability. When the control input to each muscle was 0.5, the hand was stable at the equilibrium position shown in panel (a). (S marks the shoulder joint, E the elbow, and the big open circle shows the hand position). This equilibrium position was used as a starting point for simulating various hand movements. Using the backdriving algorithm, the hand could be moved to points a and e, but not to points b, c, and d. The failure resulted because the hand stiffness became unstable during these movements. To get an insight, we plotted the joint stiffness as a function of the hand location in the workspace. (a) all the control inputs are 0.5; (b) all the control inputs are 0.2; and (c) all the control inputs are 0.8. The dark dots indicate locations where the joint stiffness is unstable, while the light dots indicate stable locations.

position is equivalent to performing the following two steps: (1) impose a passive displacement of the arm to the new position; and (2) reset the control variables so as to eliminate the induced elastic forces. Clearly, in the passive displacement, the system moves to a configuration of minimum potential energy. Then, the active change (step 2) is equivalent to finding the input pattern, which minimizes the change in potential energy with respect to the previous equilibrium.

The unstable behavior of the model system had a dramatic impact on the possibility of mapping a desired equilibrium location into a set of control variables—that is, on the possibility of implementing an equilibrium-point control. Using the backdriving algorithm, we tried to set the arm at a number of new equilibrium locations (locations a, b, c, d, and e in Figure 4a). The algorithm succeeded in finding the control patterns for the locations a and e, which fell within the stability region. However, it failed to find the appropriate controls for the positions b, c, and d, which lay inside the unstable region.

4.6. Stability Can Be Achieved by Simple Geometrical Modifications

Our first approximation of the monkey's arm geometry, led us to a model with unstable behaviors. This instability is not only undesirable for the equilibrium-point control, but it is also scarcely plausible in physiological terms: Primates are capable of maintaining stable arm postures even after deafferentation (Taub, Goldberg, & Taub, 1975; Bizzi, Accornero, Chapple, & Hogan, 1984). If stability is an important functional requirement, then it is possible to proceed in one of two al-

ternative directions: (1) with the current model structure, try to choose only those motor commands that ensure postural stability; or (2) modify the model structure in such a way that any motor command is guaranteed to generate a stable posture. The first approach leads to the complex (and not always possible) task of implementing ad hoc computational procedures capable of avoiding unstable control patterns. In contrast, the second approach relieves the motor controller from such a computational burden.

In order to correct the structure of the model, we examined the contribution of each muscle to the joint stiffness matrix, R. In our model, two conditions were always satisfied by the joint-stiffness matrix, R: (1) R was symmetric ($R_{1,2} = R_{2,1}$, for proof see Dornay, 1991b); and (2) The diagonal stiffness terms, $R_{1,1}$ and $R_{2,2}$, were larger (in absolute value) than the two-joint term, $R_{1,2}$. If the above two conditions are satisfied,[5] it can be proved (Dornay, 1991a) that *a necessary and sufficient condition for a stable joint stiffness is having stable (or negative) diagonal components,* ($R_{1,1} < 0$ and $R_{2,2} < 0$). Therefore, we only needed to consider the contributions of the muscles to the two diagonal components, $R_{1,1}$ (shoulder stiffness) and $R_{2,2}$ (elbow stiffness). Making use of eqn (5), these components can be expressed as

$$\begin{cases} R_{1,1} = \sum_{i=1}^{17} r_{1,i} \\ R_{2,2} = \sum_{i=1}^{17} r_{2,i} \end{cases}, \tag{28}$$

where we have introduced the *angular muscle stiffnesses*

$$\begin{cases} r_{1,i} = \mu_{i,1} \dfrac{\partial f_i}{\partial q_1} + \chi_{1,i} f_i \\ r_{2,i} = \mu_{i,2} \dfrac{\partial f_i}{\partial q_2} + \chi_{2,i} f_i \end{cases}, \tag{29}$$

with

$$\chi_{1,i} = \frac{\partial \mu_{i,1}}{\partial q_1}$$

$$\chi_{2,i} = \frac{\partial \mu_{i,2}}{\partial q_2}.$$

The angular muscle stiffnesses summarizes the contribution of each muscle to the shoulder and elbow joint stiffness. The coefficients, $\chi_{1,i}$ and $\chi_{2,i}$ play a major role in establishing the margin of stability of a muscle.

This point is illustrated in Figure 5, which shows the variation of the parameters related to the muscle

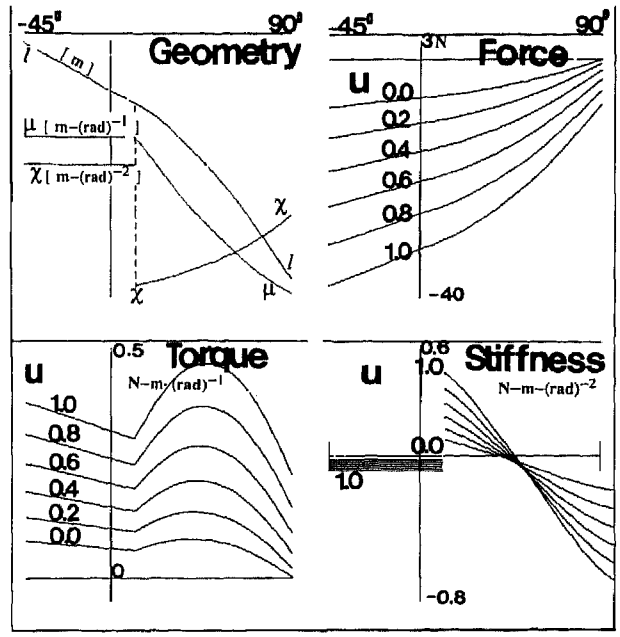

FIGURE 5. Initial stability analysis of pectoralis major capsularis. A flexion movement is shown in which the shoulder angle changes from −45° to 90°. In the Geometry panel, the muscle length, l, decreased from 8.7 cm to 4.8 cm. The moment arm of the muscle around the shoulder joint, μ, was initially constant at −1 cm∗radian^{-1}, but at q = 11° it started to decrease, eventually reaching its final value of −2.9 cm∗radian^{-1}. The moment arm derivative, χ, was zero at the first stage of the movement, jumped to −1.8 cm∗radian^{-2} at q = 11°, and then started to increase, reaching a final value of −0.75 cm∗radian^{-2}. In the Force, Torque and Stiffness panels, the behavior of the muscle is shown for six different control inputs u.

pectoralis major capsularis, as the shoulder angle changes from −45° to 90°. The model geometry of this particular muscle is also illustrated in Figure 3. The top-left panel of Figure 5 shows the plots for the muscle length, l, the moment-arm, $\mu = \partial l/\partial q$, and the coefficient $\chi = \partial \mu/\partial q$. In the first part of the shoulder-joint range, $q \in [-45°, +11°]$, the muscle is wrapped around the joint-pulley (Figure 3). Accordingly, the moment-arm is constant and $\chi = 0$. In this initial range, the force and the torque change linearly and the angular stiffness is constant and negative. The muscle contributes to stability. When the muscle becomes unwrapped from the pulley, the moment arm starts suddenly to increase (in absolute value), and χ jumps to a large negative value. At this point, the tension developed by the muscle is sufficiently large to induce a positive angular stiffness, for all the values of the control input. The muscle contributes to instability. As the joint angle keeps increasing, the rate of change of the moment arm and the muscle tension decrease. At q = 48°, the geometric stiffness contributed by χf becomes smaller than the "intrinsic stiffness," $\mu \partial f/\partial q$. As a consequence, the muscle contributes again to joint stability between 48° and 90°.

[5] These two features are in agreement with the joint-stiffness matrices measured in human subjects (Mussa-Ivaldi, Hogan, & Bizzi, 1985; Flash, & Mussa-Ivaldi, 1990).

A simple geometric modification that was sufficient to eliminate the instability of pectoralis major scapularis is shown in Figure 6. We changed the effective origin and insertion so as to keep the muscle in closer proximity to the joint. As shown in Figure 7, with this modification, the moment arm remains constant for a larger range. As the muscle becomes unwrapped, the muscle tension is small enough to maintain the angular stiffness at a negative value. Remarkably, this modification corresponded to a closer similarity between the model arm and the actual musculoskeletal geometry. Real muscles, such as the pectoralis major, do not connect the actual attachment points in a straight line, as we supposed in the initial model. Instead, connective tissues constrain the line of action of a muscle and shift its effective origin and insertion towards the center of the joint, a situation that is captured by the modified geometry of Figure 6.

Interestingly, this analysis provides a rationale for the apparent lack of efficiency of the biological design. By keeping the muscles close to a joint, their mechanical advantage is reduced. However, at the same time the stability range is substantially increased.

We repeated the above stability analysis for all the 17 muscles in the model. Then, we modified the effective origins and insertions of these muscles so as to ensure joint stability for every possible value of the control inputs. With this modification, the unstable regions of Figure 4 were completely removed. To further confirm the predicted hand stability in the modified model, we used the backdriving algorithm to derive control patterns for moving the hand to various desired equilibrium positions. For example, Figure 8 shows the outcome of the backdriving algorithm as the hand posture was smoothly shifted from an initial to a final position (Figures 8a and 8b). This equilibrium-point trajectory traversed a region that was unstable before the geometric modification of the model muscles. The control signals corresponding to the equilibrium trajectory are shown in Figure 8c. In this, as in all other tested trajectories, each signal varied continuously from an initial to a final value. Thus, by removing the instabilities from the model arm it was possible to establish a continuous mapping between equilibrium positions and muscle-control variables.

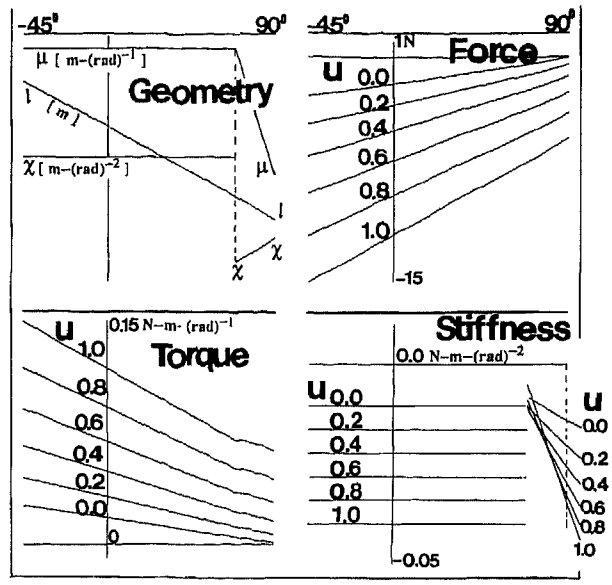

FIGURE 7. Final stability analysis of pectoralis major capsularis. The same analysis described in Fig. 5 was repeated using the "corrected" geometry shown in Fig. 6. The muscle length, l, decreased from 9.1 cm to 6.7 cm. The moment arm of the muscle around the shoulder joint, μ, was initially constant at -1 cm∗radian^{-1}, but at $q = 70°$ it started to decrease, eventually reaching its final value of -1.2 cm∗radian^{-1}. The moment arm derivative, χ, was zero at the first stage of the movement, jumped to -0.5 cm∗radian^{-2} at $q = 70°$, and then started to increase, reaching a final value of -0.39 cm∗radian^{-2}.

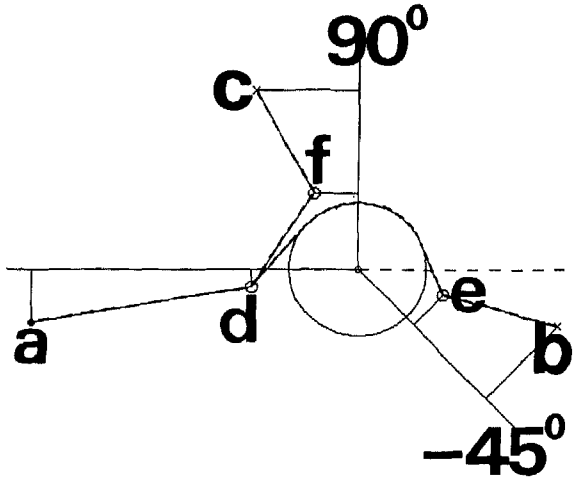

FIGURE 6. Stabilized geometric model of the shoulder flexor muscle pectoralis major capsularis. The initial geometric model was described in Fig. 3. The muscle's line of action is constrained by connective tissues represented by the effective origin d and the effective insertion e or f.

5. DISCUSSION AND CONCLUSIONS

We have investigated the relation between static stability of a limb, equilibrium-point control, and motor redundancy. Mathematically, equilibrium-point control is equivalent to the establishing of a mapping between the command signals delivered to the muscles and the equilibrium configurations of a limb.

A condition for the mapping between the command signals delivered to the muscles and the equilibrium configurations of a limb to be possible is that the limb be stable across the workspace or, more precisely, that the limb's stiffness have only negative eigenvalues. We analyzed how this condition may be translated into biomechanical constraints for single- and multi-joint limbs.

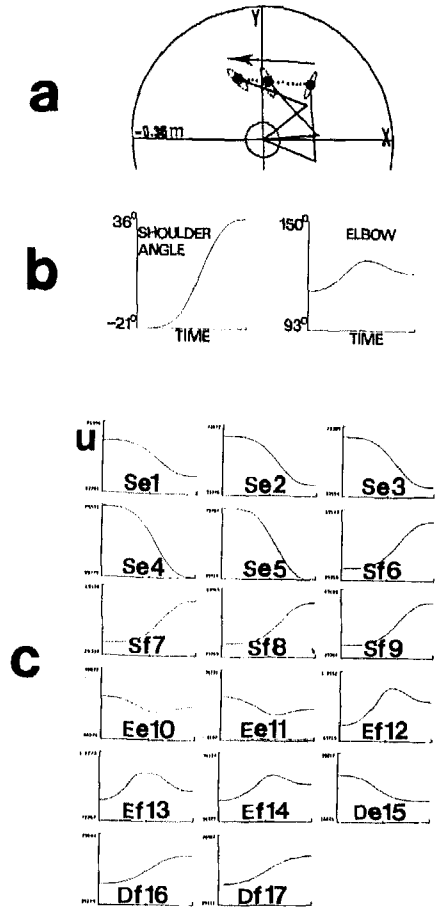

FIGURE 8. A typical equilibrium-point trajectory. The chosen hand path is a straight line with 26 intermediate points. A control input to the 17 muscles is specified for each intermediate point, defining it as an equilibrium point. The neural control input profiles for all the muscles is very smooth. When the input to a muscle reaches a minimum (0) or a maximum (1), it stays there as long as the backdriving algorithm expects it to decrease or increase, respectively. In this case other muscles take over and produce the needed change in torque. The 13th muscle shows this behavior in the middle of the movement. S = shoulder, E = elbow, D = double joint muscle, e = extensor, f = flexor muscle. The serial numbers refer to Table 1 and Table 2.

Our results indicate that the viscoelastic properties of the muscles do not provide a sufficient condition for the equilibrium-point hypothesis to be applicable. In fact, one can design single- and multi-joint systems having inherent unstable behaviors in spite of the fact that they are operated by viscoelastic muscle-like actuators. The instability of such systems arises from the fact that the moment-arms of the actuators about the joints depend upon the joint angles. The variable moment arms introduce an unstable stiffness component that may overshadow the stability provided by the viscoelastic properties of the actuators.

We studied the relation between limb stability and biomechanical constraints by developing a computer model of the primate's arm. We adopted a commonly used simplification of muscular geometry: Each model muscle acted along a straight line joining the centroid of the origin to the centroid of the insertion (Amis, Dowson, & Wright, 1979). Clearly, this geometrical representation is just a coarse approximation of the actual muscle kinematics. However, it provided us with a model in which the muscles's moment arms changed as a function of the joint angles in the same direction as the actual muscles's moment arms. For this reason, the straight-line geometry constitutes a significant improvement with respect to the more commonly adopted assumption of constant moment arms.

We estimated the origins and insertions of the model muscles by dissection and X-ray imaging of 17 arm muscles in a rhesus monkey. Then, we simulated the stability of the arm model with a variety of command inputs. Our results indicated that the straight-line muscle kinematics lead to the postural instability of the model arm in a large region of the arm's workspace. Against intuition, this instability was neither removed, nor reduced by muscle coactivation. On the contrary, we found that muscle coactivation increased the region of instability.

One effective way to remove instability from our model, was to modify the effective origins and insertions of the model muscles. More specifically, this modification corresponded approximately to the mechanical action of the tendons and connective tissues, which, in the actual arm, keep the muscles in the proximity of the joints. This result suggests that a simple design constraint rather than a dedicated control process is sufficient to ensure stability to the limb.

Recently, a similar analysis of the contribution of muscle to the joint stiffness has been made (Shadmer & Arbib, 1992). These authors proposed a second solution to the problem of instability, that of having a muscle stiffness that increases with output force. They conclude that muscle stiffness must increase linearly with muscle force to overcome the destabilizing effect of the muscle attachment geometry. This fact is evident from eqn (8): At a given joint configuration, q, the destabilizing term, γ, is linear with respect to muscle force. Because the moment arms, μ, are independent of muscle force, k must also change linearly with muscle force to counteract the changes in γ. The magnitude of the linear factor, however, is related to the distance of the muscle insertions from the joint center. Our simulations have shown that, for most of the region where there is potential instability (i.e., $\gamma > 0$), the farther the effective insertion, the greater the increase in stiffness required. Thus, having effective muscle insertions nearer to the joint center reduces the required increase in muscle stiffness in response to an increase in muscle force.

One should observe that the same design factor that ensures stability (i.e. the closeness of the muscles to the joints) is also responsible for a decrease of the joint

torque that a muscle can generate. Thus, we believe that we have found a rationale for an apparent lack of "efficiency" in the biological design.

The elimination of the possible sources of instability in the mechanical structure of the arm is crucial for solving the computational problems associated with the equilibrium-point hypothesis. For example, we considered the task of deriving a pattern of muscle activations that generates a desired equilibrium configuration of the arm. With a set of 17 muscles, this problem was severely ill-posed: The same equilibrium configuration could be achieved by infinite patterns of muscle activations.

A solution to this problem can be found by minimizing the changes in potential energy associated with the transition to a new posture (Mussa-Ivaldi, Morasso & Zaccaria, 1988; Mussa-Ivaldi, Morasso, Hogan, & Bizzi, 1991). The backdriving algorithm represents a distributed method for solving the inverse problem of muscle activations. The change of muscle activation needed to produce a given displacement could be computed by independent elements, one per muscle, each of which computes the input change necessary to cancel the change in the elastic force for that muscle induced by the passive displacement. Our simulations tested a fundamental question concerning such a distributed control system: Can the global stability of the system be assured by the stable control of the component elements? Indeed, we showed that the global stability in our system could be achieved simply by using stable component elements (muscles with stable angular stiffness).

Our results indicate that the minimum-energy principle used by the backdriving algorithm can effectively be implemented by a simulation program after all sources of local instability have been removed from the anatomical model. The inability to derive appropriate command patterns in the presence of structural instabilities is a further demonstration of the crucial role played by the biological design with respect to information processing in motor control.

REFERENCES

Amis, A. A., Dowson, D., & Wright, W. (1979). Muscle strengths and musculoskeletal geometry of the upper limb. *Engineering in Medicine*, **8**, 41–48.

An, K. N., Hui, F. C., Morrey, B. F., Linchield, R. L., & Chao, E. Y. (1981). Muscles across the elbow joint: A biomechanical analysis. *Journal of Biomechanics*, **14**, 659–669.

Bizzi, E., Accornero, N., Chapple, W., & Hogan, N. (1982). Arm trajectory formation in monkeys. *Experimental Brain Research*, **46**, 139–143.

Bizzi, E., Accornero, N., Chapple, W., & Hogan, N. (1984). Posture control and trajectory formation during arm movement. *Journal of Neuroscience*, **4**, 2738–2744.

Bizzi, E., Hogan, N., Mussa-Ivaldi, F. A., & Giszter, S. (1992). Does the nervous system use equilibrium-point control to guide single and multiple joint movements? *Behavioral and Brain Sciences*, **15**, 603–613.

Cohen, M. A., & Grossberg, S. (1983). Absolute stability of global pattern formation and parallel memory storage by competitive neural networks. *IEEE Transactions on System Man and Cybernetics*, **SMC13**, 815–825.

Colgate, J. (1988). *The control of dynamically interacting systems.* Ph.D. thesis, Department of Mechanical Engineering, MIT, Cambridge, MA.

Colgate, J., & Hogan, N. (1989). An analysis of contact instability in terms of passive physical equivalents. *Proceedings of International Conference on Robotics and Automation* (pp. 404–409). Charlottesville, VA: IEEE Press.

Dornay, M. (1991a). *Static analysis of posture and movement, using a 17-muscle model of the monkey's arm.* (Report No. TR-A-0109) *ATR Technical Report*, Kyoto, Japan.

Dornay, M. (1991b). Control of movement, postural stability, and muscle angular stiffness. *Proceedings of International Conference on Systems, Man and Cybernetics* (pp. 1373–1379). Charlottesville, Virginia: IEEE Press.

Feldman, A. G. (1966). Functional tuning of nervous system with control of movement or maintenance of a steady posture. III. Mechanographic analysis of the execution by man of the simplest motor task. *Biophysics*, **11**, 766–775.

Flanagan, J. R., Ostry, D. J., & Feldman, A. G. (1990). Control of human jaw and multi-joint arm movements In G. E. Hammond, (Ed.), *Cerebral Control of Speech and Limb Movements* (pp. 29–58). Amsterdam: Elsevier (North Holland) Science Publishers.

Flash, T. (1987). The control of hand equilibrium trajectories in multi-joint arm movements. *Biological Cybernetics*, **57**, 57–74.

Flash, T., & Mussa-Ivaldi, F. A. (1990). Human arm stiffness characteristics during the maintenance of posture. *Experimental Brain Research*, **82**, 315–326.

Goswami, A., Peshkin, M., & Colgate, J. E. (1990). Passive robotics: An exploration of mechanical computation. *IEEE International Conference on Robotics and Automation* (pp. 279–284). Cincinnati: IEEE Press.

Hoffer, J. A., & Andreassen, S. (1981). Regulation of soleus muscle stiffness in premammillary cats: Intrinsic and reflex components. *Journal of Neurophysiology*, **45**, 267–285.

Hogan, N. (1984). An organizing principle for a class of voluntary movements. *Journal of Neuroscience*, **4**, 2745–2754.

Hopfield, J. J., & Tank, D. W. (1985). Neural computation of decisions in optimization problems. *Biological Cybernetics*, **52**, 141–152.

Kelso, J. A. S., & Holt, K. G. (1980). Exploring a vibratory system analysis of human movement production. *Journal of Neurophysiology*, **43**, 1183–1196.

Latash, M. L. (1992). Independent control of joint stiffness in the framework of the equilibrium-point hypothesis. *Biological Cybernetics*, **67**, 377–384.

McIntyre, J. (1990). *Utilizing elastic system properties for the control of posture and movement.* Ph.D. thesis, Department of Brain and Cognitive Sciences, MIT, Cambridge, MA.

Mussa-Ivaldi, F. A. (1986). Compliance. In P. Morasso and V. Tagliasco, (Eds.), *Human movement understanding* (pp. 159–212). Amsterdam: North-Holland: Elsevier Science Publishers.

Mussa-Ivaldi, F. A., Hogan, N., & Bizzi, E. (1985). Neural, mechanical and geometric factors subserving arm posture in humans. *Journal of Neuroscience*, **5**, 2732–2743.

Mussa-Ivaldi, F. A., Morasso, P., & Zaccaria, R. (1988). Kinematic networks: A distributed model for representing and regularizing motor redundancy. *Biological Cybernetics*, **60**, 1–16.

Mussa-Ivaldi, F. A., Morasso, P., Hogan, N., & Bizzi, E. (1991). Network models of motor systems with many degrees of freedom. In M. D. Fraser (Ed.), *Advances in control networks and large scale parallel distributed processing models* (pp. 171–220). Norwood, NJ: Ablex Publishing Corporation.

Mussa-Ivaldi, F. A., & Hogan, N. (1991). Integrable solutions of kinematic redundancy via impedance control. *The International Journal of Robotics Research,* **10,** 481–491.

Nichols, T. R., & Houk, J. C. (1976). Improvement in linearity and regulation of stiffness that results from action of stretch reflex. *Journal of Neurophysiology,* **39,** 119–142.

Ogata, K. (1970). *Modern control engineering.* Engineering Series. Englewood Cliffs, NJ: Prentice-Hall.

Rack, P. M. H., & Westbury, D. R. (1969). The effects of length and stimulus rate on tension in isometric cat soleus muscle. *Journal of Physiology,* **204,** 443–460.

Shadmehr, R., & Arbib, M. A. (1992). A mathematical analysis of the force-stiffness characteristics of muscles in the control of a single joint system. *Biological Cybernetics,* **66,** 463–477.

Sokolnikoff, I. S., & Redheffer, R. M. (1966). *Mathematics of physics and modern engineering.* New York: McGraw Hill.

Taub, E., Golberg, I. A., & Taub, P. (1975). Deafferentation in monkeys: Pointing at a target without visual feedback. *Experimental Neurology,* **46,** 178–186.

Zeffiro, T. A. (1986). *Motor adaptations to alterations in limb mechanics.* Ph.D. thesis, Department of Brain and Cognitive Sciences, MIT, Cambridge, MA.